The variability of stomatal sensitivity to leaf water potential across tree species indicates a continuum between isohydric and anisohydric behaviours

Tamir Klein*

Institute of Botany, University of Basel, Schönbeinstrasse 6, Basel 4056, Switzerland

Summary

1. The relationship between stomatal conductance (g_s) and leaf water potential (Ψ_l) is key to the understanding of plant function under changing climate. The variability among tree species gave rise to selection towards either of two contrasting water management types: isohydric or anisohydric. This study explores the variability of g_s to Ψ_l across tree species.

2. Curves of $g_s(\Psi_l)$ were collected from the scientific literature for 70 woody plant species. The data set is comprised of angiosperm and gymnosperm species from all major forest biomes. The hypothesis that curves from different tree species diverge between isohydric and anisohydric behaviours was tested.

3. Species-specific curves formed a continuum, rather than dichotomy between isohydric and anisohydric, as confirmed by distribution models. Alternatively, the water potential at 50% of the maximum g_s ($\Psi g_s 50$) was used to quantitatively compare between species. A major difference emerged among xylem anatomy classes whereby ring-porous species had higher absolute g_s at $\Psi_l < -2$ MPa than diffuse-porous and coniferous species. A positive, linear correlation was shown between $\Psi g_s 50$ and Ψ_l at 50% loss of xylem conductivity.

4. The results suggest that stomatal sensitivity to leaf water potential strongly relates to xylem characteristics. The use of $\Psi g_s 50$ offers a quantitative alternative to the current, yet biased, distinction between isohydric and anisohydric species.

Key-words: anisohydric, drought stress, gas exchange, isohydric, stomatal conductance, xylem anatomy

Introduction

Gas exchange through leaf stomata is a fundamental phenomenon at the plant level and beyond. Its role as a major gateway between the biosphere and the atmosphere bears major implications on the global carbon and water cycles (Van der Molen *et al.* 2011; Williams *et al.* 2012). Remarkably, these several μm-scale pores can produce important feedbacks in spatial scales from ecosystems to the earth system and with temporal changes in climate. Recently, much attention was given to multiple drought-induced forest mortality events related to climate change (Allen *et al.* 2009 and references therein), raising the need to improve our understanding of tree function under water limitations. Trees can adjust their water use and hydraulic safety through the coordination of hydraulic and stomatal regulations (Sperry 2000; Brodribb & McAdam 2011; Choat *et al.* 2012). While xylem properties (e.g. conduit diameter

and pit membrane structure) provide a long-term control, stomata dynamically adjust leaf transpiration by partial closure (Tyree & Sperry 1988; Cochard, Breda & Granier 1996; Woodruff, Meinzer & Lachenbruch 2008). Upon desiccation, stomata may respond to a multitude of physical and chemical signals, including leaf hydration (turgor loss) and the xylem and foliar levels of the phytohormone abscisic acid (ABA; Brodribb & McAdam 2013, Speirs *et al.* 2013). Yet it is clear that Ψ_l is a key player in controlling guard-cell movement (Cochard, Breda & Granier 1996; Salleo *et al.* 2000; Brodribb *et al.* 2003). In fact, stomatal conductance to water vapour (g_s) and leaf water potential (Ψ_l) interact in a feedback mechanism whereby stomatal sensitivity to Ψ_l (i.e. reduction in g_s with decreasing Ψ_l) results with a consequent increase in Ψ_l (Oren *et al.* 1999; Buckley 2005).

Tardieu and Simonneau (1998) distinguished between isohydric species, where stomatal regulation maintains a fairly consistent minimum Ψ_l from day to day, and anisohydric species, where Ψ_l markedly decreases with changes

*Correspondence author. E-mail: Tamir.klein@unibas.ch

in evaporative demand. The effect of stomatal regulation (isohydric/anisohydric) on the ability of trees to survive adverse conditions has been addressed in numerous studies (e.g. West *et al.* 2007; McDowell *et al.* 2008; Bonal & Guehl 2011; Klein, Cohen & Yakir 2011; Domec & Johnson 2012). However, in spite of the many studies on the isohydric/anisohydric behaviour of trees, there is still no mathematic definition for this important plant trait. Classification into one of the two categories is usually graphically based on the relationship between g_s and Ψ_l (Fisher *et al.* 2006; McDowell *et al.* 2008). Notably, differences among species in the range of Ψ_l are mostly affected by the minimum Ψ_l value, since maximum Ψ_l is rather similar and always between 0 and -1 MPa. Therefore, potential definitions for the water management strategy (i.e. isohydric/anisohydric) can take the form of one of these alternatives: (D1) the minimum Ψ_l still permitting stomatal conductance; (D2) the slope of the change in stomatal conductance as function of Ψ_l; or (D3) the extent of variation in Ψ_l along the day. However, none of the definitions is without weaknesses. The first option requires a very unified, sensitive measurement of g_s, to account for the asymptotic behaviour of the g_s sensitivity to Ψ_l [$g_s(\Psi_l)$] approaching stomatal closure. Then, one needs to define the Ψ_l threshold between isohydric and anisohydric, which is potentially any arbitrary value between -2 MPa and -6 MPa, with little physiological meaning. The second option is complicated by the sigmoid nature of the $g_s(\Psi_l)$ curve, having a non-singular slope. The third would need to address the question of variation and delineate (arbitrarily again) a variation threshold to distinguish between the two behaviour types.

g_s integrates three different effects: (i) stomatal density over the leaf surface, that is, the number of stomata per unit leaf area; (ii) the typical stoma pore size; and (iii) the degree of aperture. Trade-offs between the different effects shaped plant life through evolution (Franks & Beerling, 2009). Notably, while the first two factors might change only on long-term time-scales ranging from weeks to plant ontogeny (and are usually species-specific), stomatal aperture is adjusted dynamically on the time-scale of minutes. Therefore, changes in g_s as function of Ψ_l largely reflect stomatal aperture, and closure, dynamics. Differences among tree species in stomatal density and typical pore size should affect the maximum g_s, where stomata are fully open. At the other end of the curve, the minimum g_s should show the species-specific epidermal or cuticular conductance, usually a minor residual of g_s.

Ψ_l is largely determined by the water potential of the surrounding air (Ψ_a; more commonly measured as vapour pressure deficit, VPD) and that of the rhizosphere (Ψ_r, often estimated from pre-dawn leaf water potential, Ψ_{pd}; Bonal & Guehl 2011). To experimentally construct a $g_s(\Psi_l)$ curve, g_s must be measured under a large range of Ψ_l values. Such range is obtained by exposing the plant to changes in the water potentials of the air, the rhizosphere or both. This can be achieved experimentally by a drying procedure or by measuring Ψ_l and g_s under decreasing Ψ_a (increasing VPD) or decreasing Ψ_{pd}. Stomata are highly sensitive to Ψ_l, but also respond to changes in other environmental factors, for example CO_2 concentration, air temperature and light. Therefore, to relate changes in g_s to changes in Ψ_l, all other factors must be kept constant. Clearly, an experimental approach is advantageous here, yet limited in the technical aspects of controlling the environment over mature trees and also limited in the transferability of the results back to the field. Repeating coupled measurements of Ψ_l and g_s during sunny days with similar air temperatures and light levels can produce a robust $g_s(\Psi_l)$ curve. In addition, $g_s(\Psi_l)$ is not a state function, and curve hysteresis was shown (Blackman, Brodribb & Jordan, 2009; Brodribb & McAdam 2013). While significant hysteresis was shown in *Pinus radiata*, in other species it was minor compared to the difference between the species-specific curves (Blackman, Brodribb & Jordan 2009), or even negligible (e.g. for *Calitris rhomboidea*; Brodribb & McAdam, 2013).

In this synthesis study, curves of stomatal sensitivity to leaf water potential [gs(Ψl)] were collected from the scientific literature into a data set of 70 woody species from all major forest biomes. Subsequently, the data set was used to test the hypothesis that curves from different tree species diverge between isohydric and anisohydric regulation of stomatal conductance.

Materials and methods

DATA COLLECTION

Curves of stomatal sensitivity to leaf water potential were collected from the scientific literature according to the following criteria: (i) the response measured was stomatal conductance (g_s, in mol m^{-2} s^{-1}) *per se* and not leaf hydraulic conductivity (K_{leaf}) or transpiration (T). One exception was made where g_s was readily calculated from values of T and a given vapour pressure deficit (VPD; Blackman, Brodribb & Jordan, 2009). (ii) g_s was related to simultaneous measurements of leaf water potential (Ψ_l, usually at midday, i.e. Ψ_{md}), that is, curves relating g_s to pre-dawn leaf water potential (Ψ_{pd}) were not used. (iii) All data were empirically observed. Simulated curves were not used.

Data mining and screening according to the aforementioned criteria yielded $g_s(\Psi_l)$ curves for 66 woody plant species: 56 trees, 8 shrubs and 2 lianas. All major forest biomes were represented by angiosperm species (61). Data on gymnosperm species were scarcer, potentially due to objective difficulties in measuring g_s of coniferous needles. Therefore, published data were complemented by *ad hoc* measurements of four additional coniferous species performed by the author, yielding a total number of 70 species in the data set (Table S1, Supporting information). The large number of data sources meant some variation in measurement conditions among the different curves. The time of measurement during the day, air temperature (T_{air}), photosynthetic photon flux density (PPFD), VPD and Ψ_{pd} of each curve were included in the data set wherever reported at the source studies or could be reconstructed from other reliable data. Out of the 70 species, information on time of measurement, T_{air}, PPFD, VPD and Ψ_{pd} was available for 66, 66, 59, 37 and 42 species, respectively. Examination of the reported measurement conditions showed that 98% of the 70 curves were measured between high morning and afternoon

(9:00–16:00; mostly around midday), 77% were always measured at $T_{air} \geq 20$ °C, and 64% always at PPFD≥ 300 μmol m^{-2} s^{-1}. Atmospheric CO_2 concentration was ambient and kept at 390 ± 50 p.p.m. in all studies. On this rather standard background, there were large variations in VPD and Ψ_{pd} among species, and also individually for each species. Twenty-five curves included measurements at VPD increasing above 3 kPa, and 21 curves at Ψ_{pd} decreasing below -1 MPa, of which ten with both high VPD and low Ψ_{pd}. Additional sixteen curves were measured in dehydration or soil-drying experiments. This showed that the range of g_s values in each curve related to changes in water availability, rather than changes in other factors, such as atmospheric CO_2 concentration, temperature or light conditions.

ADDITIONAL CHARACTERIZATION OF SPECIES INCLUDED IN THE DATA SET

In addition to plant form and biome, which were reported for the species in their respective studies, information on other water-use-related traits was collected from external data sources. The xylem anatomy type of each species was determined using Schweingruber (1990), The Xylem data base (http://www.wsl.ch/dendro/xylemdb/) and the Inside Wood data base (Wheeler 2011; http://insidewood.lib.ncsu.edu/search), supplemented by personal communication with F.H. Schweingruber for species that were not described there. The sensitivity of xylem conductivity to water potential was characterized by the water potential at 50% loss of xylem conductivity ($\Psi PLC50$), reported in Choat *et al.* (2012). In total, wood anatomy and $\Psi PLC50$ were characterized for 59 and 31 species, respectively.

DATA ANALYSIS

To examine the utility of the potential definitions of isohydric/anisohydric behaviour (D1–D3, see Introduction), species-specific curves were used to calculate: (i) the leaf water potential at 25% of the maximum stomatal conductance ($\Psi g_s 25$), capturing the minimum Ψ_l of the linear portion of the $g_s(\Psi_l)$ curve; (ii) the difference $\Psi g_s 75 - \Psi g_s 25$, capturing the entire linear portion of the curve; and (iii) the daily range of $\Psi_{pd} - \Psi_{md}$, where reported as Ψ_{pd} and Ψ_{md} that were measured on the same day or from daily curves of Ψ_l. Species-specific values for these three parameters, corresponding with the definitions D1–D3, were plotted for 57, 56 and 25 species, depending on the source data. For each parameter, a distribution histogram was built with JMP software (Cary, NC, USA) and was fitted with the six best-fitting distribution models, including the normal-two-mixture distribution, to test the hypothesis of two contrasting behaviours, that is, isohydric/anisohydric. The likelihood of each distribution model was tested by the corrected Akaike Information Criterion, given by: AICc = $-2\log(\text{likelihood}) + 2k + 2k(k+1)/(n-k-1)$, where k is the number of parameters in the model and n is the sample size. The goodness-of-fit was tested for the best-fitting model, using the Shapiro–Wilk W test for normal and generalized logarithm distributions, and the Kolmogorov's D test for log-normal distribution.

To quantitatively compare between species, leaf water potential at 50% of the maximum stomatal conductance ($\Psi g_s 50$) was calculated from species-specific curves, as previously demonstrated (Brodribb *et al.* 2003; Hao *et al.* 2010). A data set of $\Psi g_s 50$ values was prepared (Table S1). $\Psi g_s 50$ values were analysed by ANOVA with growth form, xylem anatomy type and forest biome as factors. Differences between responses were considered significant when type 3 sum of squares met the F-test criterion at probability <0·05. Means were compared using Student's t-test, reported as letters indicating significant differences in Figure 3. In addition to the ANOVA, $\Psi g_s 50$ values were correlated with species-specific

values of water potential at 50% loss of xylem hydraulic conductivity ($\Psi PLC50$) and linear regression was calculated.

Results and discussion

RELATIONSHIP BETWEEN STOMATAL CONDUCTANCE AND LEAF WATER POTENTIAL

Among the 70 species-specific curves included in the data set, 65 curves followed the expected sigmoid function for the relationship between g_s and Ψ_l ($(g_s = g_{s\,max}/(1 + (\Psi_l/\Psi g_s 50)^a)$, after Guyot, Scoffoni & Sack, 2011), where g_s gradually decreased from a maximum value at $-1 > \Psi_l > 0$ MPa to its minimum value at a more negative Ψ_l (Fig. 1a). Five species, however, had a bell-shaped curve, where maximum g_s was recorded at intermediate, rather than mild Ψ_l (*Fagus sylvatica* in Aranda, Gil & Pardos, 2000; *Laurus nobilis* in Salleo *et al.* 2000; *Ceratonia siliqua*, *Quercus suber* and *Olea oleaster* in Lo Gullo *et al.* 2003). In addition to the challenges of constructing any $g_s(\Psi_l)$ curve (see Introduction), this meta-analysis combined different curves from different studies that had no standard protocol for measurement conditions. The bell-shaped curves from those reports were prepared by pooling data from different seasons (Aranda, Gil & Pardos, 2000; Lo Gullo *et al.* 2003) or experiments (Salleo *et al.* 2000), and hence, other factors came to play, for example low light levels limiting g_s at mild Ψ_l.

Overall, g_s ranged between 0·94 and 0 mol m^{-2} s^{-1}, at $0 < \Psi_l < -7·0$ MPa, with the majority of curves at $g_s < 0·5$ mol m^{-2} s^{-1} and $\Psi_l < -4·0$ MPa. Across species, gas
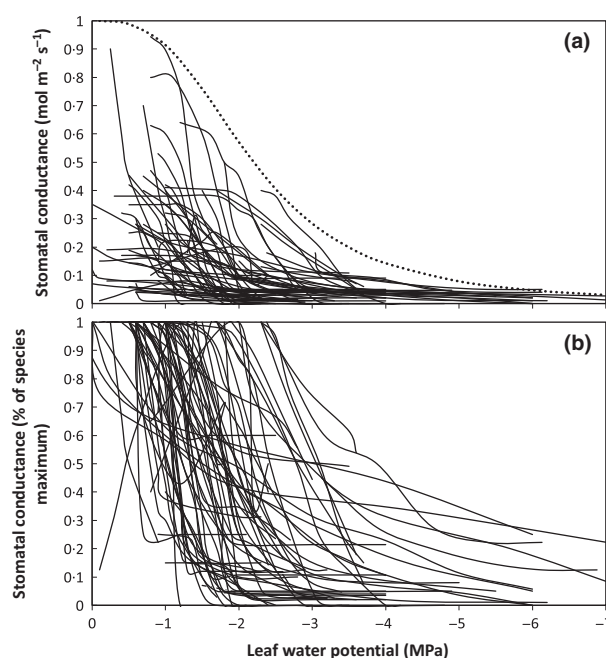

Fig. 1. Absolute (a) and relative (b) stomatal conductance (g_s) as function of leaf water potential (Ψ_l) for 70 tree species. The dotted curve is the theoretical function $g_s = 1/(1 + (\Psi_l/-2·2)^3)$ describing the physiological boundary for maximum g_s as function of Ψ_l.

exchange mostly occurred at a relatively narrow range between −1·0 and −2·0 MPa, with much lower conductance already at −3·0 MPa. Using the data set, a boundary-line analysis assigned the values $g_{s\ max} = 1·0$ mol m^{-2} s^{-1}, $\Psi g_s 50 = -2·2$ MPa and $a = 3$ in the sigmoid function $g_s = 1/(1 + (\Psi_l/-2·2)^3)$ (Fig. 1a). There was a distinction between a cluster of curves for the majority of species, with $g_s \leq 0·2$ mol m^{-2} s^{-1} at $\Psi_l < -2$ MPa, and curves from seven species maintaining $g_s > 0·22$ mol m^{-2} s^{-1} at −2·0 MPa: *Pistacia lentiscus*, *Hymenaea courbaril*, *Quercus oleoides*, *Q. frainetto*, *Q. pubescens*, *Q. macroplepis* and *Q. petraea* (Fig. 1a). Curves from this small subset of species not only had lower Ψ_l values, but also seemed to shift the operational Ψ_l range some 0·5–1·5 MPa into the more negative part of the graph. To explain this pattern, knowledge of the tree functional groups was explored.

TESTING THE ISOHYDRIC/ANISOHYDRIC FRAMEWORK

The relationship between the relative, species-dependent g_s and Ψ_l (Fig. 1b) yielded a large range of species-specific curves. Differences in the stability of Ψ_l, which are used to distinguish between isohydric and anisohydric plant species, are mostly affected by the minimum Ψ_l value, since maximum Ψ_l is rather similar among species and mostly between 0 and −1 MPa. Therefore, the relationship between g_s and Ψ_l was used as proxy for the water management strategy identification. Within the observed large range of $g_s(\Psi_l)$ curves, no clear divergence emerged, but rather a continuum of leaf responses.

Species-specific $g_s(\Psi_l)$ curves were further analysed to examine the utility of the potential definitions of isohydric/anisohydric behaviour. Theoretically, anisohydric plants should diverge from isohydric by having a lower Ψ_l still permitting stomatal conductance (D1), a lower slope of the curve (D2) or a higher variation in Ψ_l along the day (D3). Due to the sigmoidal nature of $g_s(\Psi_l)$, calculations were made on the linear portion of each curve: D1 was tested by the leaf water potential at 25% of the maximum stomatal conductance ($\Psi g_s 25$, Fig. 2a) and D2 by the difference $\Psi g_s 75 - \Psi g_s 25$ (Fig. 2b). D3 was tested by the maximum range of $\Psi_{pd} - \Psi_{md}$ within one day, reported for 25 of the species (Fig. 2c). If an isohydric/anisohydric dichotomy existed, it should have been demonstrated as a step-change in at least one of the bar graphs describing each of the three parameters (Fig. 2a-c). Instead, all three parameters showed a continuum of responses and lack of grouping. Across species, $\Psi g_s 25$, $\Psi g_s 75 - \Psi g_s 25$ and $\Psi_{pd} - \Psi_{md}$ changed in a gradual manner. The only exception was excessively large $\Psi g_s 75 - \Psi g_s 25$ ranges of two species: 5·70 and 6·30 for *Enchylaena tomentosa* and *Atriplex vesicaria*, respectively, both are semi-arid shrubs living on the dry edge of plant life. To further test the extent of isohydric/anisohydric divergence, distribution histograms (insets in Fig. 2a–c) were fitted with the six best-fitting distribution models, including the normal-two-mixture distribution, that is, assuming divergence into two distribution groups.
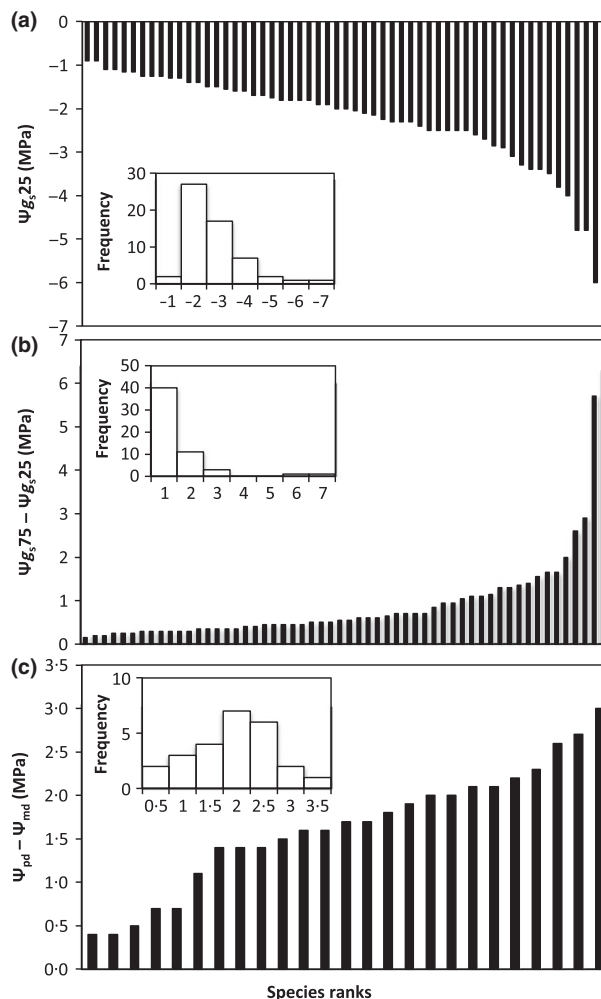

Fig. 2. The distribution of parameters associated with isohydric/anisohydric behaviour across the woody species in the data set: (a) leaf water potential (Ψ_l) at 25% stomatal conductance ($\Psi g_s 25$); (b) the difference in Ψ_l at 75% and 25% stomatal conductance; and (c) the difference between Ψ_l between pre-dawn and midday ($\Psi_{pd} - \Psi_{md}$). Each bar represents one species with available data. The corresponding distribution plots are presented in the *insets*.

Table 1 shows that the normal-two-mixture distribution was not the best-fitting model for any of the three parameters, having consistently higher AICc values than those of the best-fitting model. The goodness-of-fit of the best-fitting distribution models for the three parameters was confirmed using the appropriate statistical tests (Table 1).

DIFFERENCES AMONG FUNCTIONAL GROUPS, ANATOMICAL TYPES AND FOREST BIOMES

As an alternative for the isohydric/anisohydric framework, the water potential at 50% of the maximum stomatal conductance ($\Psi g_s 50$) was used to quantitatively compare between species (Table S1). While $\Psi g_s 50$ was arbitrarily determined, it contains valuable information about the water potential at which a certain species operates under rather standard conditions (between high morning and

Table 1. The likelihood of the normal-two-mixture model and the best-fitting model for the distribution of three parameters associated with the isohydric/anisohydric behaviour (Fig. 2): the leaf water potential (Ψ_l) at 25% of the maximum stomatal conductance ($\Psi g_s 25$); the difference between Ψ_l at 75% and 25% of the maximum stomatal conductance ($\Psi g_s 75 - \Psi g_s 25$); and the daily range of Ψ_l between pre-dawn and midday ($\Psi_{pd} - \Psi_{md}$). Likelihood was tested by the corrected Akaike Information Criterion, where smaller values indicate better model fits. The goodness-of-fit was tested for the best-fitting model, using the Shapiro–Wilk W test for normal and generalized logarithm distributions, and the Kolmogorov's D test for log-normal distribution. $P > 0.05$ confirms the null hypothesis that the data are from the distribution model under test

Model	$\Psi g_s 25$	$\Psi g_s 75 -$ $\Psi g_s 25$	$\Psi_{pd} - \Psi_{md}$
Normal-two-mixture	171·3	125·3	59·6
Generalized logarithm	159·3	–	–
Log-normal	–	90·1	–
Normal	–	–	57·3
Goodness-of-fit	$P < W$ 0·4543	$P > D$ 0·0693	$P < W$ 0·4764

Fig. 3. Variations in leaf water potential at 50% stomatal conductance ($\Psi g_s 50$) as function of xylem anatomy type (a) and forest biome (b). Biomes are tropical (Tr), tropical seasonal (Trs), temperate (Te), Mediterranean (M) and semi-arid (SA). Letters indicate significant ($P < 0.05$) differences between xylem types or biomes. *Error bars* represent the standard error of the mean. See Supporting Information Table S1 for specific data.

afternoon, at $T_{air} \geq 20$ °C and PPFD≥ 300 µmol m^{-2} s^{-1}), with some degree of air or soil drying. ANOVA showed that there was no difference between trees ($\Psi g_s 50 = -1.9 \pm 0.1$ MPa) and shrubs ($\Psi g_s 50 = -2.1 \pm 0.2$ MPa; $P = 0.4$). A major difference emerged among xylem anatomy classes whereby ring-porous species had higher stomatal conductance at low water potentials than diffuse-porous ($P = 0.016$; Fig. 3a). In the data set, eight species were identified as ring-porous: *Pistacia lentiscus, Prunus dulcis, Quercus faginea, Q. frainetto, Q. pubescens, Q. petraea, Tamarix ramosissima* and *Vitis vinifera*. Their mean $\Psi g_s 50$ was -2.47 MPa (-2.69 MPa excluding *Vitis vinifera*). *Quercus, Pinus* and *Ficus* were the three genera with more than two species in the data set, and their mean $\Psi g_s 50$ was $-2.87, -1.60$ and -1.38 MPa, respectively, indicating lower stomatal sensitivity to water potential in the oaks. Among the seven species maintaining $g_s > 0.25$ mol m^{-2} s^{-1} at -2.3 MPa (Fig. 1a), four were ring-porous and only one was diffuse-porous. These trees produce large vessels early in the growth season (forming an annual ring) that have the highest hydraulic conductivity among all tree species, allowing for increased capacity to maintain maximum stomatal conductance under developing water potential gradient (Panshin & de Zeeuw 1980; Wheeler, Bass & Rodgers 2007). Nevertheless, the large vessels are very sensitive to cavitation and lose functionality later in the season, when moisture decreases and narrower conduits are formed to take their place in the sap flow. The shift in the operational Ψ_l range of ring-porous species can therefore be seen as part of a strategy that sacrifices xylem safety in favour of high gas-exchange activity, in agreement with earlier reports (Sperry *et al.* 1994; McCulloh *et al.* 2010).
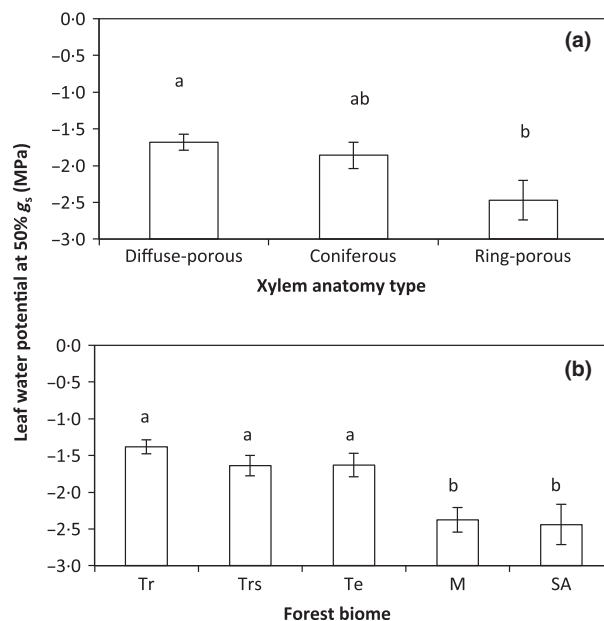
Among different biomes, trees from Mediterranean forests and semi-arid woodlands had significantly lower $\Psi g_s 50$ than trees from tropical and temperate forests ($P < 0.0001$; Fig. 3b; boreal forest excluded due to low sample size). In xeric environments, trees are exposed to higher VPD than in mesic sites and hence must experience lower Ψ_l. This means that in order to maintain an equivalent level of gas exchange, trees in Mediterranean and semi-arid sites must shift the stomatal sensitivity threshold towards more negative values than in tropical and temperate sites. A similar pattern was identified comparing provenances of a pine species growing in common garden plots along a precipitation gradient (Klein *et al.* 2012). The hydraulic conductance of the leaf usually scales with g_s (Zhang *et al.* 2013), yet species with low $\Psi g_s 50$ have shown to increase their hydraulic conductance as water availability increased, an important process during recovery (Blackman, Brodribb & Jordan, 2009; Domec & Johnson 2012). If, for example, the Mediterranean *Pinus halepensis* ($\Psi g_s 50 = -1.80$) followed the $g_s(\Psi_l)$ curve of the temperate *Pinus radiata* ($\Psi g_s 50 = -1.05$, reaching minimum g_s at $\Psi_l = -2.0$ MPa), stomata would have been shut for 4 months in sequence and for most of the day during additional 4 months. This is because Ψ_l of *P. halepensis* in its native habitat is constantly below -2.0 MPa throughout the dry summer (Klein *et al.* 2013). This does not mean that stomatal regulation of trees in the drier biomes is less conservative than in the more humid biomes. In terms of absolute g_s (Fig. 1a), most curves fit in the main cluster, where $g_s \leq 0.2$ mol m^{-2} s^{-1} at $\Psi_l < -2$ MPa. Species of the

different biomes mostly moved along the same curve, albeit populated different segments of this curve: while mesic trees produced high g_s at high Ψ_l, xeric species were characterized by low g_s at low Ψ_l.

RELATIONSHIP BETWEEN STOMATAL SENSITIVITY TO WATER POTENTIAL AND TO LEAF HYDRATION

During leaf desiccation, stomatal closure usually correlates with the turgor loss point (Ψ_{TLP}) of the leaves and the movement of ions across the guard-cell membranes (Brodribb *et al.* 2003, 2003). Leaf traits such as size, texture, petiole's vessel diameter and hydraulic conductivity, and Ψ_{TLP} are therefore essential to the understanding of differential stomatal behaviours among species (Hao *et al.* 2010). For the majority of species in the data set, leaf traits and hydration status were not reported. However, for eight tropical dry forest trees, Brodribb *et al.* (2003) showed a significant linear regression between $\Psi g_s 50$ and Ψ_{TLP}. Comparing ten tropical *Ficus* species, the water potential difference between $\Psi g_s 50$ and Ψ_{TLP} increased with $\Psi g_s 50$ (Hao *et al.* 2010). In both studies, $\Psi g_s 50$ was usually 0·1–0·4 MPa higher than Ψ_{TLP}, suggesting that the trigger for initial closure involves other signals. Stomatal closure is also regulated by foliar and xylem levels of the phytohormone abscisic acid (ABA; Brodribb & McAdam 2013, Speirs *et al.* 2013), which diverge among species. Complex interactions between leaf hydration, ABA signals and xylem properties can also generate some plasticity to the $g_s(\Psi_l)$ curve. During recovery, hysteresis can be significant (e.g. in *Pinus radiata*; Brodribb & McAdam, 2013), but is usually minor (Blackman, Brodribb & Jordan, 2009). The curves reported here (Fig. 1) represent a dehydration response (i.e. plants subjected to desiccation or measured during the transition from wet to dry season), and therefore, the corresponding rehydration curves, whether similar or divergent, deserve an independent examination.

RELATIONSHIP BETWEEN STOMATAL SENSITIVITY TO WATER POTENTIAL AND TO VPD

Stomata are highly sensitive to fluctuations in VPD, and g_s decreases with increasing VPD (Bonal & Guehl, 2011). Oren *et al.* (1999) showed that at low VPD, tree species and individuals with high g_s show higher sensitivity to VPD than those with lower g_s, as required by the role of stomata in regulating Ψ_l. As a result, g_s of different trees tend to converge at high VPD. The results from the current data set seem to show a similar trend for g_s with decreasing Ψ_l. However, due to the heterogeneity of atmospheric conditions in which measurements were performed, a conclusion cannot be drawn. With eight species from each xylem anatomy class, data in Oren *et al.* (1999) show that conifers had lower g_s and hence significantly lower sensitivity to VPD than vessel-bearing angiosperms ($P = 0.05$). Differences between stomatal sensitivity to Ψ_l and to VPD probably involve additional factors. Ψ_l might

decrease without any increase in VPD, for example, due to decrease in root water potential (Ψ_r). Interspecific differences in root accessibility to soil water can therefore account for a difference in Ψ_l at the same VPD.

RELATIONSHIP BETWEEN STOMATAL AND XYLEM SENSITIVITY TO WATER POTENTIAL

Among the 70 species in the data set, 31 have a known empirical value of water potential at 50% loss of xylem conductivity ($\Psi PLC50$). $\Psi g_s 50$ values were correlated with species-specific $\Psi PLC50$ as a measure of the stem (and branch) xylem vulnerability to cavitation. To minimize the effect of species with extreme water potential tolerance, the regression was restricted to $\Psi PLC50 > -8·0$ MPa and $\Psi g_s 50 > -3·3$ MPa. This analysis yielded a cluster of 27 data-points showing a significant, positive, linear correlation ($r^2 = 0·41$, $P = 0·0003$) and four outliers (Fig. 4). Among the different xylem anatomy types, vessel-bearing angiosperms (diffuse- and ring-porous species) seemed to distribute well around this correlation, whereas coniferous species had similarly moderate $\Psi PLC50$ and $\Psi g_s 50$. The two outlier data-points at the very negative, far left end of the plot are the semi-arid *Calitris rhomboidea* and the Mediterranean *Ceratonia siliqua*, both among the most cavitation-resistant tree species known. The two other outliers, namely the semi-arid *Tamarix ramosissima* and the Mediterranean *Quercus ilex,* seem to maintain g_s beyond $\Psi PLC50$. The exceptionally risky behaviour of these two species (and the very safe behaviour of the other three) is also evident from very narrow (wide, for the latter) hydraulic safety margins (Choat *et al.* 2012). $\Psi g_s 50$ and $\Psi PLC50$ changed between $-0·5$ and $-3·1$ MPa, and between $-0·6$ and $-7·2$ MPa, respectively. This suggested that, across species, the range of $\Psi g_s 50$ was more conservative than that of $\Psi PLC50$: differences between species in stomatal sensitivity to water potential were smaller than
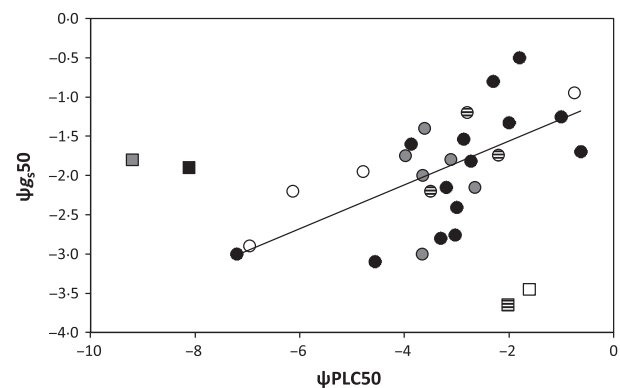

Fig. 4. Relationship between leaf water potential at 50% stomatal conductance ($\Psi g_s 50$) and leaf water potential at 50% loss of hydraulic conductivity ($\Psi PLC50$) for 27 tree species (diffuse-porous, black; ring-porous, white; coniferous, grey; undefined, hatched). Circles represent species included in the linear regression ($\Psi g_s 50 = 0·49 \times \Psi PLC50 - 0·42$); Outliers denoted by square symbols.

the differences in xylem sensitivity. This was largely related to the fact that resistant species (having more negative ΨPLC50) had larger hydraulic safety margin than sensitive ones. Based on analysis of data available from Choat *et al.* (2012), the hydraulic safety margin tends to increase linearly from ca. 0·8 MPa to 1·8 MPa for tree species with ΨPLC50 of −4·0 and −6·0 MPa, respectively.

The regression equation $\Psi g_s 50 = 0·28 \times \Psi PLC50 − 1·0$ MPa defines the interdependence between stomatal regulation and xylem functionality (Fig. 4). This regression was applicable to vessel-bearing angiosperms but not to conifers, possibly due to the smaller number of species, all from the Pinaceae. Most tree species adjusted their stomatal gas exchange around a Ψ_l value, which was ca. half the Ψ_l that causes 50% loss of xylem conductivity. This was mostly in agreement with results of a comparative study on eight tree species in a tropical, seasonally dry forest (Brodribb *et al.* 2003), also showing some flexibility in the linkage between $\Psi g_s 50$ and ΨPLC50. Reconstructing the correlation between $\Psi g_s 50$ and ΨPLC50 from that study yielded the regression equation $\Psi g_s 50 = 0·63 \times \Psi PLC50 − 0·10$ MPa, with $r^2 = 0·48$, however, not significant ($P = 0·06$) due to the smaller sample size. The positive, linear correlation here supports the hypothesis of Cochard, Breda and Granier (1996), Tyree and Sperry (1988), Sperry (2000) and others that stomata regulate leaf water potential to avoid xylem cavitation. This is also in agreement with the observation that g_s is positively correlated with stem water status in fourteen different tree species (Zhang *et al.* 2013).

CONCLUDING REMARKS AND IMPLICATIONS ON FORESTS UNDER CLIMATE CHANGE

The use of $\Psi g_s 50$ offers a quantitative alternative to the current, yet biased, distinction between isohydric and anisohydric species. Species-specific curves formed a continuum, rather than dichotomy between isohydric and anisohydric. This is of particular importance considering the expectation for higher frequency of drought events in many regions world-wide (Alpert *et al.* 2006; Zhang *et al.* 2007), in turn inducing lower Ψ_l. The results also suggest that stomatal sensitivity to leaf water potential relates to xylem properties such as xylem anatomy type and xylem sensitivity to cavitation. Yet the current analysis is inconclusive regarding such effects. Studying 22 temperate deciduous woody species from SE USA, Hoffmann *et al.* (2011) showed a significant decrease in the slope of $g_s(\Psi_l)$ as wood density increases among species. Considering the observations of lower $\Psi g_s 50$ in ring-porous species and oaks reported here, this might indicate an effect of additional xylem properties, for example vessel diameter.

The preliminary observation of higher g_s at low Ψ_l in ring-porous species compared to diffuse-porous and coniferous species can bear major implications to forest species composition. Scaling of the stomatal regulation must consider additional eco-physiological determinants, such as leaf phenology, root/shoot ratio, stand density. But if ring-porous species maintain high gas exchange under dry conditions, they can have a major advantage in the forest interspecies competition, either directly (higher growth) or indirectly (seizure of water resources). Kolb and Stone (2000) showed consistently higher photosynthesis rates in ring-porous oak compared to coexisting pine in an upland forest in Arizona, USA. At the drought limit, however, where water availability is strongly limiting, such water-spending behaviour could prove unsustainable. One case study comparing water use in coexisting Mediterranean pine and oak species showed how pines, and not oaks, extended their growth into semi-arid sites (Klein *et al.* 2013). Oak species were also found less desirable than coexisting diffuse-porous species (*Ceratonia siliqua*, *Olea oleaster*) for afforestation in drier parts of the Mediterranean (Lo Gullo *et al.* 2003). Among 88 reported cases of drought- and heat-induced tree die-off in multiple locations across the globe (Allen *et al.* 2010), ten involved ring-porous species, such as *Carya*, *Celtis*, *Fraxinus* and *Quercus* spp. Whether this reflects a higher frequency of tree mortality in ring-porous species vs. other classes is unknown and requires more data on the species occurrence. Future research should further explore the consequences of xylem anatomy on stomatal regulation from the tree level to the forest scale.

References

Allen, C.D., Macalady, A.K., Chenchouni, H., Bachelet, D., McDowell, N., Vennetier, M. *et al.* (2009) A global overview of drought and heat-induced tree mortality reveals emerging climate change risks for forests. *Forest Ecology and Management*, **259**, 660–684.

Alpert, P., Baldi, M., Ilani, R., Krichak, S., Price, C., Rodo, X. *et al.* (2006) Relations between climate variability in the Mediterranean region and the tropics: ENSO, South Asian and African monsoons, hurricanes and Saharan dust. *Developments in Earth and Environmental Sciences*, **4**, 149–177.

Aranda, I., Gil, L. & Pardos, J.A. (2000) Water relations and gas exchange in *Fagus sylvatica* L. and *Quercus petraea* (Mattuschka) Liebl. In a mixed stand at their southern limit of distribution in Europe. *Trees*, **14**, 344–352.

Blackman, C.J., Brodribb, T.J. & Jordan, G.J. (2009) Leaf hydraulics and drought stress: response, recovery and survivorship in four woody temperate plant species. *Plant, Cell & Environment*, **32**, 1584–1595.

Bonal, D. & Guehl, J.-M. (2011) Contrasting patterns of leaf water potential and gas exchange responses to drought in seedlings of tropical rainforest species. *Functional Ecology*, **15**, 490–496.

Brodribb, T.J. & McAdam, S.A.M. (2011) Passive origins of stomatal control in vascular plants. *Science*, **331**, 582–585.

Brodribb, T.J. & McAdam, S.A.M. (2013) Abscisic acid mediates a divergence in the drought response of two conifers. *Plant Physiology*, **162**, 1370–1377.

Brodribb, T.J., Holbrook, N.M., Edwards, E.J. & Gutierrez, M.V. (2003) Relations between stomatal closure, leaf turgor and xylem vulnerability in eight tropical dry forest trees. *Plant, Cell & Environment*, **26**, 443–450.

Buckley, T.N. (2005) The control of stomata by water balance. *New Phytologist*, **168**, 275–292.

Choat, B., Jansen, S., Brodribb, T.J., Cochard, H., Delzon, S., Bhaskar, R. *et al.* (2012) Global convergence in the vulnerability of forests to drought. *Nature*, **491**, 752–755.

Cochard, H., Breda, N. & Granier, A. (1996) Whole tree hydraulic conductance and water loss regulation in *Quercus* during drought: evidence for stomatal control of embolism? *Annals of Forest Science*, **53**, 197–206.

Domec, J.C. & Johnson, D.M. (2012) Does homeostasis or disturbance of homeostasis in minimum leaf water potential explain the isohydric versus anisohydric behavior of *Vitis vinifera* L. cultivars? *Tree Physiology*, **32**, 245–248.

Fisher, R.A., Williams, M., Do Vale, R.L., Da Costa, A.L. & Meir, P. (2006) Evidence from Amazonian forests is consistent with isohydric control of leaf water potential. *Plant, Cell & Environment*, **29**, 151–165.

Franks, P.J. & Beerling, D.J. (2009) Maximum leaf conductance driven by CO2 effects on stomatal size and density over geologic time. *Proceedings of the National Academy of Sciences USA*, **106**, 10343–10347.

Guyot, G., Scoffoni, C. & Sack, L. (2011) Combined impacts of irradiance and dehydration on leaf hydraulic conductance: insights into vulnerability and stomatal control. *Plant, Cell & Environment*, **35**, 857–871.

Hao, G.-Y., Sack, L., Wang, A.-Y., Cao, K.-F. & Goldstein, G. (2010) Differentiation in leaf water flux and drought tolerance traits in hemiepiphytic and non-hemiepiphytic *Ficus* tree species. *Functional Ecology*, **24**, 731–740.

Klein, T., Cohen, S. & Yakir, D. (2011) Hydraulic adjustments underlying drought resistance of *Pinus halepensis*. *Tree Physiology*, **31**, 637–648.

Klein, T., Di Matteo, G., Rotenberg, E., Cohen, S. & Yakir, D. (2012) Differential ecophysiological response of a major Mediterranean pine species across a climatic gradient. *Tree Physiology*, **33**, 26–36.

Klein, T., Shpringer, I., Fikler, B., Elbaz, G., Cohen, S. & Yakir, D. (2013) Relationship between stomatal regulation, water-use, and water-use efficiency of two coexisting key Mediterranean tree species. *Forest Ecology and Management*, **302**, 34–42.

Kolb, T.E. & Stone, J.E. (2000) Differences in leaf gas exchange and water relations among species and tree sizes in an Arizona pine-oak forest. *Tree Physiology*, **20**, 1–12.

Lo Gullo, M.A., Salleo, S., Rosso, R. & Trifilo, P. (2003) Drought resistance of 2-year-old saplings of Mediterranean forest trees in the field: relations between water relations, hydraulics and productivity. *Plant and Soil*, **250**, 259–272.

McCulloh, K., Sperry, J.S., Lachenbruch, B., Meinzer, F.C., Reich, P.B. & Voelker, S. (2010) Moving water well: comparing hydraulic efficiency in twigs and trunks of coniferous, ring-porous, and diffuse-porous saplings from temperate and tropical forests. *New Phytologist*, **186**, 439–450.

McDowell, N.G., Pockman, W.T., Allen, C.D., Breshears, D.D., Cobb, N., Kolb, T.E. *et al.* (2008) Mechanisms of plant survival and mortality during drought: why do some plants survive while others succumb to drought? *New Phytologist*, **178**, 719–739.

Oren, R., Sperry, J.S., Katul, G.G., Pataki, D.E., Ewers, B.E., Phillips, N. *et al.* (1999) Survey and synthesis of intra- and interspecific variation in stomatal sensitivity to vapour pressure deficit. *Plant, Cell & Environment*, **22**, 1515–1526.

Panshin, A.J. & de Zeeuw, C. (1980) *Textbook of Wood Technology*. McGraw-Hill, New York, USA.

Salleo, S., Nardini, A., Pitt, F. & Lo Gullo, M.A. (2000) Xylem cavitation and hydraulic control of stomatal conductance in Laurel (*Laurus nobilis* L.). *Plant, Cell & Environment*, **23**, 71–79.

Schweingruber, F.H. (1990) *Anatomy of European Woods*. WSL, Birmensdorf, Haupt, Bern, and Stuttgart.

Speirs, J., Binney, A., Collins, M., Edwards, E. & Loveys, B. (2013) Expression of ABA synthesis and metabolism genes under different irrigation strategies and atmospheric VPDs is associated with stomatal conductance in grapevine (*Vitis vinifera* L. cv Cabernet Sauvignon). *Journal of Experimental Botany*, **64**, 1907–1916.

Sperry, J.S. (2000) Hydraulic constraints on plant gas exchange. *Agricultural and Forest Meteorology*, **104**, 13–23.

Sperry, J.S., Nichols, K.L., Sullivan, J.E.M. & Eastlack, S.E. (1994) Xylem embolism in ring-porous, diffuse-porous, and coniferous trees of Northern Utah and Interior Alaska. *Ecology*, **75**, 1736–1752.

Tardieu, F. & Simonneau, T. (1998) Variability among species of stomatal control under fluctuating soil water status and evaporative demand: modelling isohydric and anisohydric behaviours. *Journal of Experimental Botany*, **49**, 419–432.

Tyree, M.T. & Sperry, J.S. (1988) Do woody plants operate near the point of catastrophic xylem dysfunction caused by dynamic water stress? answers from a model. *Plant Physiology*, **88**, 574–580.

Van der Molen, M.K., Dolman, A.J., Ciais, P., Eglin, T., Gobron, N., Law, B.E. *et al.* (2011) Drought and ecosystem carbon cycling. *Agricultural and Forest Meteorology*, **151**, 765–773.

West, A.G., Hultine, K.R., Jackson, T.L. & Ehleringer, J.R. (2007) Differential summer water use by *Pinus edulis* and *Juniperus osteosperma* reflects contrasting hydraulic characteristics. *Tree Physiology*, **27**, 1711–1720.

Wheeler, E.A. (2011) InsideWood – a web resource for hardwood anatomy. *IAWA Journal*, **32**, 199–211.

Wheeler, E.A., Bass, P. & Rodgers, S. (2007) Variations in dicot wood anatomy: a global analysis based on the insidewood database. *IAWA Journal*, **28**, 229–258.

Williams, C.A., Reichstein, M., Buchmann, N., Baldocchi, D., Beer, C., Schwalm, C. *et al.* (2012) Climate and vegetation controls on the surface water balance: synthesis of evapotranspiration measured across a global network of flux towers. *Water Resources Research*, **48**, W06523.

Woodruff, D.R., Meinzer, F.C. & Lachenbruch, B. (2008) Height-related trends in leaf xylem anatomy and shoot hydraulic characteristics in a tall conifer: safety versus efficiency in water transport. *New Phytologist*, **180**, 990–999.

Zhang, X., Zwiers, F.W., Hegerl, G.C., Lambert, H.L., Gillett, N.P., Solomon, S. *et al.* (2007) Detection of human influence on twentieth-century precipitation trends. *Nature*, **448**, 461–465.

Zhang, Y.-J., Meinzer, F.C., Qi, J.-H., Goldstein, G. & Cao, K.-F. (2013) Midday stomatal conductance is more related to stem rather than leaf water status in subtropical deciduous and evergreen broadleaf trees. *Plant, Cell & Environment*, **36**, 149–158.

Supporting Information

Additional Supporting information may be found in the online version of this article:

Table S1. Water potential at 50% of the maximum stomatal conductance for 70 woody plant species, including species-specific ancillary data.